Attenuation Coefficient Measurement Technique at 100 MHz with the Scanning Laser Acoustic Microscope

KALERVO M. U. TERVOLA, STEVEN G. FOSTER, AND
WILLIAM D. O'BRIEN, JR, SENIOR MEMBER, IEEE

Abstract—**There has been a lack of an accurate procedure for the measurement of an attenuation coefficient for biological tissues at 100 MHz with the scanning laser acoustic microscope (SLAM). The solution to this problem has been approached with two general schemes. One involved a calibrated look-up table, and the other utilized the measurement of insertion loss. For the latter a procedure has been developed and verified using known biological solutions. The insertion loss procedure yields an attenuation coefficient uncertainty to within five percent, a dynamic range from 4 to 28 dB/mm, and an insertion loss sensitivity of 0.2 dB.**

I. Introduction

AN IMPORTANT tissue characterization property is the ultrasonic attenuation coefficient, which is the decrease in energy of the sound wave when it propagates through a material. The attenuation includes absorption and scattering. Absorption represents the loss of energy into heat within the specimen. Scattering is a redirection of the energy due to the inhomogeneities of the specimen and includes reflection, refraction, and diffraction. The scanning laser acoustic microscope (SLAM) is a useful tool for providing at 100 MHz, the ultrasonic attenuation coefficient of tissue. A number of techniques have been developed to perform this measurement with the SLAM, and this report details and evaluates these techniques. Details of ultrasonic velocity measurements are found in companion papers [1], [2].

When the SLAM is in the interference mode, it produces an interferogram image of equal phase wavefronts on a TV monitor. One of the earliest attenuation coefficient measurement techniques relied upon the operator's subjective opinion of the overall brightness on the monitor of the interference-mode image [3]. The insertion loss was determined by visually examining the interferogram image and by assessing when the interference lines disappeared, which was caused by reducing the transducer's driving voltage with a calibrated electrical attenuator. The attenuator was located between the ultrasonic driver and the transducer. This process was repeated with and without the specimen in place, and the difference in readings of the calibrated attenuator yielded the insertion loss. This procedure relied greatly upon operator experience. In general, each of the two insertion loss measurements had an uncertainty of ± 3 dB.

The same technique has also been evaluated when the acoustic microscope displayed the acoustic image on the monitor. Generally, the light and dark areas in the acoustic image correspond to areas with low or high ultrasonic attenuation levels in the object, respectively. There are difficulties in using the acoustic image to determine the ultrasonic attenuation coefficient because the system is not linear, the signal-to-noise (S/N) ratio is low, and the acoustic illumination is not uniform. These problems are not as severe for the electronically generated interference lines. Therefore, it has not been possible to determine accurately the specimen's attenuation coefficient from the acoustic image. Thus this procedure has not been seriously pursued.

One of the first attempts to improve the procedures and minimize some of these problems involved the digitization and storage of the SLAM's video signal [4]. The first application of this capability involved the development of a calibration curve, or "look-up" table, from which the insertion loss could be determined. The utilization of this procedure was extremely difficult because a different look-up table had to be generated for each location on the image, which was due to its nonuniformity [5].

A more generalized insertion loss procedure has been developed. It involves the comparison of two received signal amplitudes, one with and the other without a specimen of known thickness inserted in the sound path. Fig. 1 schematically depicts the regression analysis line of the insertion loss method, which may be derived from insertion loss values for a range of thicknesses of the same specimen. The slope of the line yields the attenuation coefficient and the intercept represents the attenuation due to reflective losses.

This report details the measurement of the ultrasonic

Manuscript received April 1984; revised September 1984. This work was supported in part by the U.S. National Institutes of Health under Grants CA 36029 and AM 21557 and in part by the Academy of Finland.

K. M. U. Tervola is with the Department of Electrical Engineering, University of Oulu, SF 90570 Oulu 57, Finland.

S. G. Foster is with Therm-X, Inc., 701 Devonshire Drive, Bldg. B1 #10, Champaign, IL 61820, USA.

W. D. O'Brien, Jr. is with the Bioacoustics Research Laboratory, Department of Electrical and Computer Engineering, University of Illinois, 1406 Green St., Urbana, IL 61801, USA.

0018-9537/85/0300-0259$01.00 © 1985 IEEE

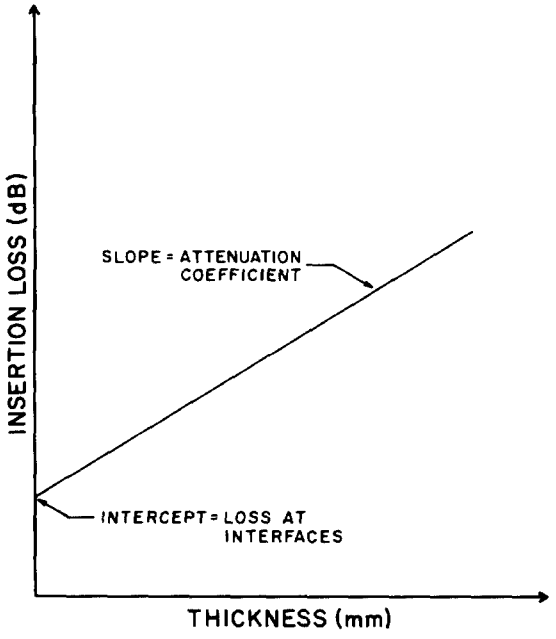

Fig. 1. Schematic representation of a regression analysis line of insertion loss versus specimen thickness to determine the ultrasonic attenuation coefficient.

attenuation coefficient with the SLAM. There are only a few reports on the attenuation coefficient measurement at 100 MHz of biological tissues [3], [6]. With this improved and well-documented technique, it is hoped that our understanding of ultrasonic attenuation at this high frequency will be greatly improved with the development of a reliable database.

II. Basic Operating Principles

Two main components are required to determine the ultrasonic attenuation coefficient: the microscope itself and a computer system. Fig. 2 schematically shows the block diagram of the whole system. Detailed descriptions of the SLAM operation have been published [7]–[11] as well as those of the interface with the computer system [1], [4]. Therefore, only the germane features will be presented.

Briefly, the specimen under investigation is positioned between the fused-silica stage and the gold-coated surface of the coverslip. The specimen is acoustically illuminated with an incident ultrasonic plane wave. The acoustic image information is contained on the lower surface of the coverslip and is extracted by means of a scanning laser beam. The amount of reflected laser light that is detected by the photodiode is proportional to the localized tilt of the coverslip surface, which in turn relates to the localized acoustic pressure variations in the specimen. The modulated laser light is detected by the wideband photodiode, demodulated, and then displayed as an acoustical image on a monitor.

The electronic interface between the SLAM and the 32-bit Perkin-Elmer minicomputer was designed and constructed in-house [4]. This data acquisition system provides the capability to extract digitally the image and other numerical data for signal and image processing. No modifications to SLAM were required to implement this scheme. Three signals are provided to the data acquisition system, *viz.*, horizontal and vertical sync and the acoustic image video signal. The video signal is amplified by an RF amplifier, which is local to the SLAM, and transmitted to the analog–digital (A/D) converter, which is local to the computer. The accuracy of the conversion is eight bits, and the sampling frequency is approximately 30 MHz, with a dynamic range of ± 500 mV. The whole image (all 482 raster lines) is digitized line by line with 1514 data points per raster line. The specimen area (field of view) under investigation is 3×2 mm, which yields an individual pixel size of about 2 μm horizontally $\times$ 4 μm vertically, respectively. The wavelength in soft tissues at 100 MHz is about 15 μm, and the resolution of the system is about 20 μm. Due to the relatively high attenuation in soft tissues at 100 MHz, the specimen thickness is generally less than 1 mm. To improve the S/N ratio, the system utilizes averaging since the noise is Gaussian distributed. When the entire image is digitized, the maximum number of sample measurements at each point could not exceed 64 because of the limited amount of memory in the present system.

For insertion loss measurements the incident ultrasonic amplitude is precisely varied. The system contains precision electrical attenuators (0–70 dB in 0.1-dB steps) such that a known amount of attenuation between the 100-MHz signal source and the ultrasonic transducer (see Fig. 2) may be introduced.

III. Evaluation of Error Sources

The principal technical difficulties in measuring the attenuation coefficient accurately and precisely with SLAM are its nonlinearity, low S/N ratio, nonuniform illumination of the specimen, and reference level variation with the signal level. Each of these problems is discussed subsequently.

To measure the linearity characteristics of the system, a very thin layer of saline (a few micrometers) was placed between the fused-silica stage and the coverslip. The receiver gain was then adjusted to use the full range of the A/D converter. The decrease of the acoustic image video signal P_x was recorded as a function of electrical attenuation inserted between the ultrasonic driver and the transducer. The amplitude P_0 of this basic illumination was recorded at an inserted attenuation of zero. The measurement results are shown in Fig. 3 in which the no specimen video signal output

$$V_{dB} = 20 \log (P_x/P_0) \tag{1}$$

is plotted as a function of the inserted electrical attenuation. The reference level variation of the video signal was not taken into account for these measurements, but was considered later. The linearity characteristics of this data set were studied using a least-squares fit algorithm. If the system had been perfectly linear, then both the slope and correlation coefficient would have had unity. This was not

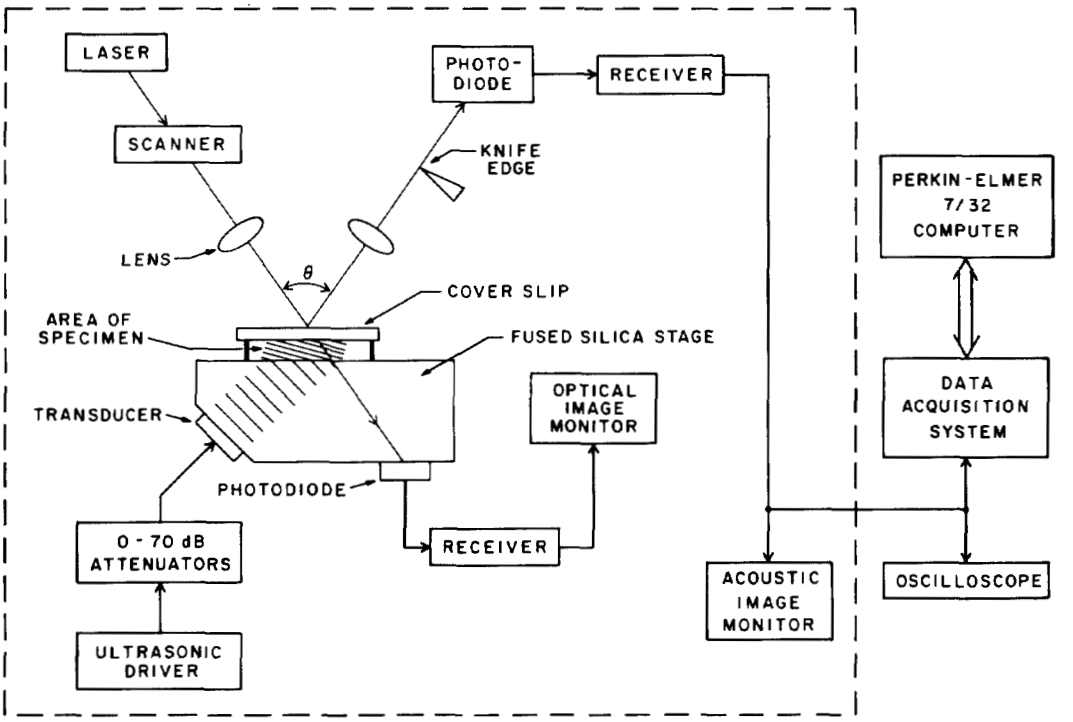

Fig. 2. Block diagram of the SLAM (within the dashed boundary) and the computer system.

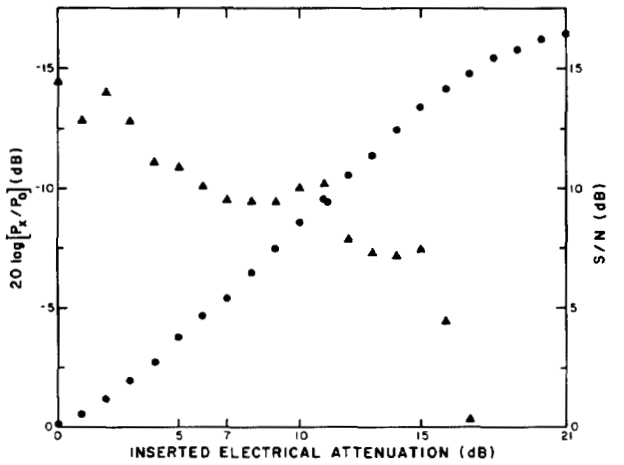

Fig. 3. No specimen video signal output denoted by (•) and signal-to-noise ratio (▲) as a function of the inserted electrical attenuation. The reference level variation with the video signal level was not taken into account for these measurement.

TABLE I
SLOPE OF THE ACOUSTIC IMAGE VIDEO SIGNAL VERSUS INSERTED ELECTRICAL ATTENUATION AND ITS CORRELATION COEFFICIENT AS A FUNCTION OF VARIOUS INSERTED ELECTRICAL ATTENUATION RANGES

Electrical Attenuation Range (dB)	Reference Level Uncorrected		Reference Level Corrected	
	Slope	Correlation coefficient	Slope	Correlation coefficient
0-12	0.90	0.9974	0.94	0.9990
1-12	0.92	0.9985	0.96	0.9991
2-12	0.94	0.9990	0.97	0.9991
3-12	0.96	0.9993	0.99	0.9996
4-12	0.97	0.9993	1.00	0.9998
5-12	0.97	0.9990	1.00	0.9998
6-12	1.00	0.9991	1.00	0.9997
7-12	1.03	0.9999	1.01	0.9995

[a]A very thin (a few micrometers) layer of saline served as the specimen. Two cases are shown, one where the reference level was not taken into account, and the other where it was.

the case, as can be seen from the results in Table I, where the slope and the correlation coefficient (for the uncorrected reference level) are listed as a function of the inserted attenuation. Table I shows that the linearity improves as the attenuation range (that is, the dynamic range) decreases. The most linear region appears to be from 6 to 12 dB for this data set.

To assess the S/N ratio, the amplitude distribution of one pixel in the middle of the acoustic image is first evaluated. The same thin layer of saline is used. The amplitude of the basic illumination P_0 in that pixel is sampled 10 000 times over a time period of 17 min, and its probability distribution is shown in Fig. 4 together with the best-fit Gaussian distribution. To test the quality of the Gaussian distribution fit, a χ^2 test was performed using 24 degrees of freedom. This yielded a χ^2 value of 32.06 when the normalized values less than 0.1 were ignored. The χ^2 value for 24 degrees of freedom and for a critical value of 0.1 is 33.2. Thus, the hypothesis that the data were obtained from sampling a Gaussian distribution is substantiated. The individual sources of noise could not be assessed because the individual components within the microscope could not be accessed.

The determination of the S/N ratio is based on the model

$$v = s + n \tag{2}$$

where v is the actual, sampled signal, s is the pure signal

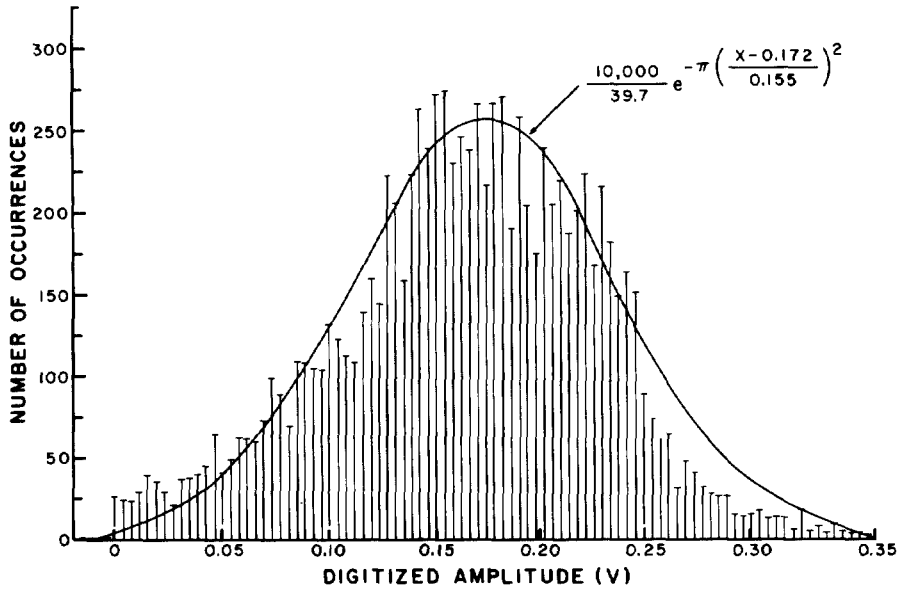

Fig. 4. Amplitude distribution of one pixel taken over a 17-minute time period. The solid line represents a best-fit Gaussian distribution.

(without noise), and n is the noise signal. Since the noise is Gaussian distributed, and it is assumed that s and n are independent, the signal s can be approximated by averaging v many times; in our case a single raster line of 1514 data points in the middle of the acoustic image was averaged 512 times, yielding

$$s(k) = (1/512) \sum_{i=1}^{512} v_i(k), \qquad k = 1, 1514. \tag{3}$$

The noise signal n is the difference between the signal v and the result of averaging just once; that is

$$n(k) = v(k) - s(k), \qquad k = 1, 1514. \tag{4}$$

The powers of the noise signal N and the signal S are determined from

$$N = (1/1514) \sum_k n(k)^2 - [(1/1514) \sum_k n(k)]^2, \qquad k = 1, 1514, \tag{5}$$

and

$$S = (1/1514) \sum_k s(k)^2 - [(1/1514) \sum_k s(k)]^2, \qquad k = 1, 1514, \tag{6}$$

thus yielding the S/N ratio, which is shown in Fig. 3, as a function of the inserted electrical attenuation. The best result of 14 dB is achieved at the zero electrical attenuation level. The poorest S/N value in the most linear range (from 6 to 12 dB) is about 7 dB. It should be noted that there is a trade-off in that the best S/N ratio is not necessarily found under the most linear conditions.

The nonuniformity of the basic illumination image (zero inserted attenuation) is illustrated in Figs. 5 and 6. Fig. 5 is a photograph of the entire imaging area (3 × 2 mm) taken directly from the SLAM's monitor and qualitatively

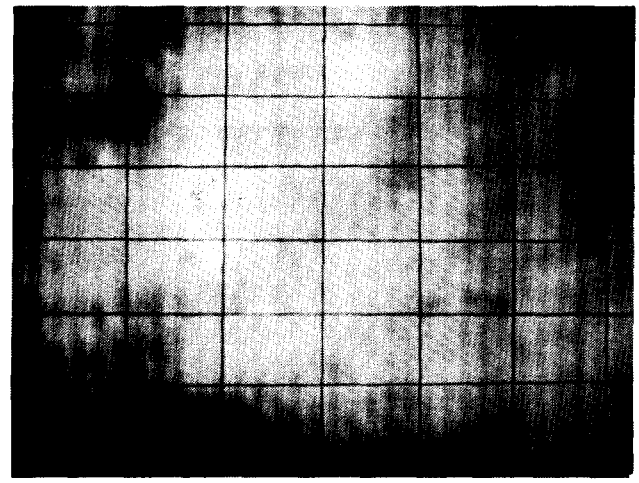

Fig. 5. A photograph of an acoustic image from the SLAM's monitor, demonstrating the nonuniform illumination. The specimen is a very thin layer of saline.

shows the nonuniform acoustic illumination. A very thin layer of saline served as the specimen. By subdividing the image into 8 × 8 subdivisions, each of which is about 375 μm horizontally and 250 μm vertically, the degree of uniformity is improved within each subdivision as contrasted to the entire image. This will be pursued further in order to compensate for nonuniform illumination.

Fig. 6 shows three amplitude profiles of a raster line taken from the middle of the image. Two recordings are taken through a very thin layer of saline for different receiver gain settings and one with air as the specimen. The raster signal consists of three regions: the specimen video signal is denoted by the symbol s, the backtrace signal by b, and a waiting period by w. The amplitude range of the saline signals is quite appreciable and means that the whole imaging area cannot be used in the insertion loss measurement.

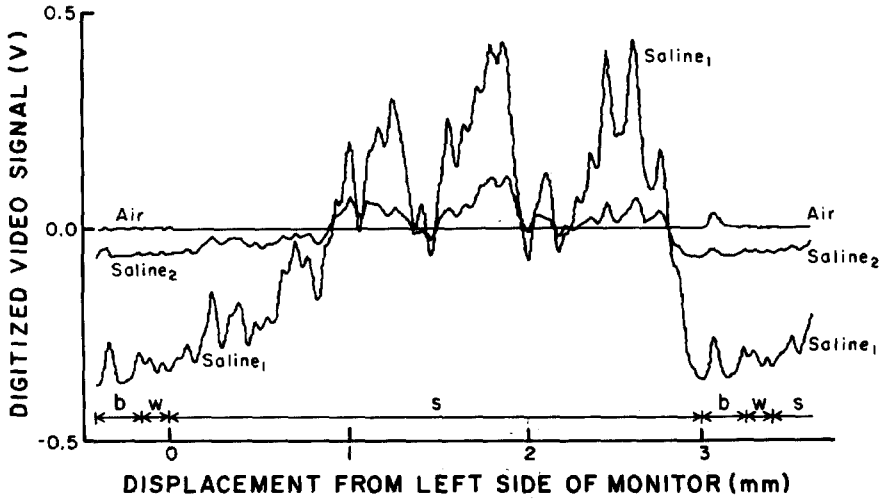

Fig. 6. Digitized video signals of one raster line when saline (at two different receiver gain settings) or air is used as the specimen. The reference level is measured during the backtrace (denoted by *b*) and then there is a wait period (*w*) before the specimen video signal (*s*). Each raster line was averaged 1024 times.

The recording through air stays at a level of zero in the *s* range of Fig. 6 because air is acoustically opaque. Note that the reference signal amplitude (*b* range) is the same. For the two saline traces the reference level changes. This is not surprising because a video amplifier is probably not DC coupled. However, it must be accounted for in terms of attenuation measurements because a good reference signal is required.

IV. Attenuation Coefficient Technique

Due to the nonuniformity of the image, the use of the entire 3 × 2 mm image would yield variable attenuation coefficient results across the image. As suggested from Fig. 5, the use of one of the 8 × 8 subimages would improve the uniformity. Therefore, the image is subdivided into 64 subimages (375 μm × 250 μm or 192 × 60 pixels) to improve image uniformity for calculating the ultrasonic attenuation coefficient.

To account for the change of the reference level with varying signal level, the reference level (*b* range in Fig. 6) and appropriate signal level (*s* range) are captured from the same raster line. The average reference level is determined by using 152 samples of the backtrace signal, which then is used as the reference voltage $R(y)$ for that raster line. The voltage V for one of the 64 subimages is calculated in a 11520-point array according to the expression

$$V = 1/(11520)\left[\sum_{x=K}^{K+191}\sum_{y=L}^{L+59}(v(x,y) - R(y))^2\right]^{1/2} \quad (7)$$

where x and y are the horizontal and vertical direction indices, respectively, and $v(x, y)$ is the voltage of pixel (x, y). Indices K and L choose one of the 64 subimages.

To demonstrate the improvement in the system's linear characteristics, the decrease of the basic illumination as a function of the attenuation level is measured again by accounting for the reference level change (Fig. 7). The measurement was performed in exactly the same way as in Fig. 3. The slope of the curve and its correlation coefficient as a function of the range of the inserted electrical attenuation are listed in Table I. The data indicate that the system has a nearly linear response in the range from 0 to 12 dB, which means that the useful dynamic range has been improved.

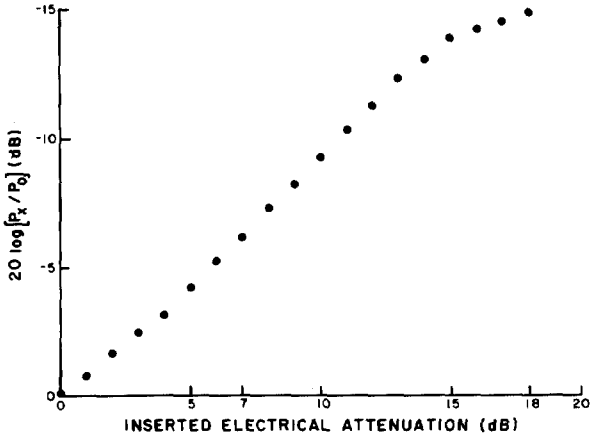

Fig. 7. No specimen video signal output (equation (7)) as a function of the inserted electrical attenuation. The reference level variation with the video signal level was taken into account for these measurements.

Up to now, all measurements have been made without a biological specimen on the microscope stage; that is, a drop of saline was used to couple the coverslip to the microscope stage. A specially designed arrangement for biological specimens has been devised in order to make the appropriate insertion loss measurements as a function of specimen thickness in as short a time period as possible. The placement of the objects on the microscope stage is shown schematically in Fig. 8. To avoid changes in the measurement system while replacing the object, various thicknesses of the object are placed on the stage at the same time. In general, the arrangement is such that there

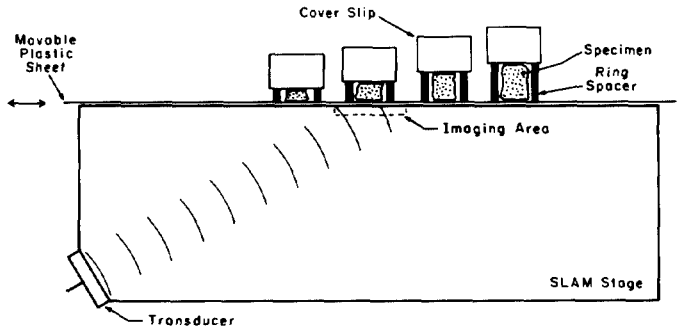

Fig. 8. Placement of the objects on the acoustic microscope stage.

are four different thicknesses of the same specimen. The specimens are placed on a plastic sheet that provides a movable platform so that a specimen can be easily positioned over the imaging area. Examination of the plastic sheet material has shown that it does not affect the illumination uniformity of the sound field.

The measurement of the insertion loss values is as follows. The movable plastic sheet is shifted so that only saline is positioned in the imaging area (not shown in Fig. 8). The wavefield amplitude in saline V_0 is measured and recorded. The plastic sheet is moved so that the specimen is positioned in the imaging area, and then the value V_x for the wavefield amplitude, which has passed through the specimen, is recorded. The insertion loss (IL) is evaluated using (1), where P_0 and P_x are V_0 and V_x, respectively, and are each determined by (7). The insertion loss is determined four times for each of the specimen thicknesses. If the system were linear, then the attenuation coefficient could be determined directly by applying a least-squares fit algorithm to the insertion loss versus thickness data. But, because of the nonlinear system behavior, a calibration curve is determined instead. The calibration curve is a plot of V_0, the wavefield amplitude through saline in dB and determined according to (1), versus the inserted electrical attenuation. The calibration curve slope is used as a correction for the nonlinearity to yield the ultrasonic attenuation coefficient A according to the expression

$$A = A_{\text{raw}}/\beta \tag{8}$$

where A_{raw} is the attenuation coefficient of the specimen determined directly from the insertion loss versus thickness slope and β is the correction term determined from the slope of the calibration curve. An example of this procedure is given in the next section.

V. Evaluation

To evaluate the technique for measuring the attenuation coefficient, aqueous solutions of bovine serum albumin (BSA) fraction V were used because its attenuation coefficient at 100 MHz and at 20°C has been independently determined [12]. Precise solution concentrations of BSA were made by dissolving a known weight of BSA powder into a known volume of distilled water. Following the insertion loss measurements the BSA concentration was measured by evaporating a known amount of BSA solution and weighing the remaining material. The BSA concentrations were 0.055 g/ml and 0.096 g/ml, which have attenuation coefficients at 100 MHz and 20°C of 3.60 and 4.67 dB/mm, respectively, according to [12]. Thus, the evaluation of the attenuation coefficient measurement technique can be performed for attenuation coefficient values near 4 dB/mm. The temperature during the course of these measurements was estimated to be between 20 and 21°C.

TABLE II
Ultrasonic Attenuation Coefficient Data of Aqueous Solutions of Bovine Serum Albumin Taken on the Scanning Laser Acoustic Microscope at 100 MHz

BSA solution concentration = 0.055 gm/ml[a]

Thickness (mm)	Insertion Loss (dB) 1	2	3	4
1.15	−1.3	−1.4	−1.5	−1.4
1.56	−3.0	−2.6	−3.1	−3.0
2.41	−5.3	−4.7	−4.9	−4.9
3.71	−7.1	−6.5	−6.6	−6.4

BSA solution concentration = 0.096 gm/ml[b]

Thickness (mm)	Insertion Loss (db) 1	2	3	4
1.15	−2.0	−2.3	−2.3	−2.0
1.56	−3.7	−3.7	−3.6	−3.6
2.41	−6.8	−6.7	−6.5	−6.6
3.71	−9.3	−9.2	−9.2	−9.3

[a] A_{raw} = 2.54 dB/mm and β = 0.74.
[b] A_{raw} = 3.51 dB/mm and β = 0.78.

The ultrasonic attenuation coefficient measurement data at 100 MHz for the two solution concentrations of BSA are shown in Table II. Four thicknesses of 1.15, 1.56, 2.41, and 3.17 mm were used, and four insertion loss values were recorded for each thickness. The thickness of each specimen was determined by the height of the ring spacer, which was accurately measured with a micrometer. For each concentration a least-squares algorithm fits the 16 insertion loss values at their respective thickness to a straight line. The slope of the two concentrations yields A_{raw}; that is, 2.54 dB/mm for C = 0.055 gm/ml and 3.51 dB/mm for C = 0.096 gm/ml. Also, for each measurement series the slopes of the calibration curve β yield for each concentration 0.74 and 0.78. Therefore, from (8) the ultrasonic attenuation coefficients at 100 MHz for these two BSA concentrations are 3.43 and 4.50 dB/mm, respectively, which are within five percent of the published values [12].

The sensitivity of the system was determined using the same experimental conditions as those described for the linearity measurements. The system responded to a 0.2 dB change in the adjustment of the attenuators at attenuation levels from 0 to 15 dB.

VI. Discussion

To determine the ultrasonic attenuation coefficient of soft tissue at 100 MHz with the SLAM, the insertion loss range should be within the 0 to 15 dB range, where the linearity is optimal. The sound field uniformity under the no specimen condition is quite good within one of the 64 subimages because both the S/N ratio and the uniformity are at their best in the middle of the imaging area. The best range for the insertion loss measurements according to linearity is from 5 to 12 dB, but the average S/N ratio is better in the range from 0 to 7 dB. The BSA solution measurements were performed in the range from 1 to 10 dB, where the uncertainty of the attenuation coefficient measurement appears to be within five percent. The precision of the insertion loss measurements appears to be better than ± 0.1 dB, and the sensitivity in the insertion loss measurements was better than 0.2 dB in the range of 0 to 15 dB. The dynamic range of the attenuation coefficient measurements was determined elsewhere [13] to be about 24 dB/mm; that is, from 4 to 28 dB/mm. The upper limit was derived using rat liver specimens that were of 370, 550, 740, and 920 μm thick. Thinner specimens than those used in BSA solution measurements were required for these measurements because the attenuation coefficient is higher for rat liver than for BSA solutions used in this study.

Acknowledgments

Our sincere thanks go to both sides of the Atlantic Ocean. The support of the UHB-Research Group, University of Oulu, Finland, and the enthusiastic atmosphere of the Bioacoustics Research Laboratory, University of Illinois, are gratefully appreciated.

References

[1] P. M. Embree, S. G. Foster, G. Bright, and W. D. O'Brien, Jr., "Ultrasonic velocity spatial distribution analysis of biological materials with the scanning laser acoustic microscope," in *Acoustical Imaging*. New York: Plenum, 1983, vol. 13, pp. 203-216.

[2] P. M. Embree, K. M. U. Tervola, S. G. Foster, and W. D. O'Brien, Jr., "Spatial distribution of the speed of sound in biological materials with the scanning laser acoustic microscope," *IEEE Trans. Sonics Ultrason.*, SU-32, no. 2, Mar. 1984. See page 000 of this TRANSACTIONS.

[3] J. D. Pohlhammer, C. A. Edwards, and W. D. O'Brien, Jr., "Phase insensitive ultrasonic attenuation coefficient determination of fresh bovine liver over an extended frequency range," *Med. Phys.*, vol. 8, no. 5, pp. 692-694, Sept. 1981.

[4] S. G. Foster, "An image digitizing system for scanning laser acoustic microscope," M.S. Thesis, Department of Electrical Engineering, University of Illinois at Urbana-Champaign, IL, 1981.

[5] A. M. Mravca, "Semi-automated techniques to measure ultrasonic propagation properties using a scanning laser acoustic microscope," M.S. Thesis, Department of Electrical Engineering, University of Illinois at Urbana-Champaign, IL, 1981.

[6] D. E. Yuhas and L. W. Kessler, "Acoustic microscopic analysis of myocardium," in *Ultrasonic Tissue Characterization II*, M. Linzer, Ed. Washington, DC: U.S. Government Printing Office, National Bureau of Standards, spec. pub. 515, pp. 73-79, 1979.

[7] A. Korpel, L. W. Kessler, and P. R. Palermo, "An acoustic microscope operating at 100 MHz," *Nature*, vol. 232, pp. 110-111, 1971.

[8] ——, "Simultaneous acoustic and optical microscopy of biological specimens," *Nature*, vol. 239, pp. 111-112, 1972.

[9] ——, "Practical high Resolution acoustic microscopy," in *Acoustical Holography*, vol. 4, G. Wade, Ed. New York: Plenum Press, 1972.

[10] ——, "Recent Developments with the scanning laser acoustic microscope," in *Acoustical Holography*, vol. 5, P. S. Green, Ed. New York: Plenum, 1974, pp. 15-23.

[11] L. W. Kessler, "The sonomicroscope," in *Proc. 1974 IEEE Ultrason. Symp.*, IEEE cat no. 74-CHO-896-1 SU, pp. 735-737.

[12] L. W. Kessler and F. Dunn, "Ultrasonic investigation of the conformal changes of bovine serum albumin in aqueous solution," *J. Phys. Chem.*, vol. 73, pp. 4256-4263, 1969.

[13] K. M. U. Tervola, M. A. Grummer, J. W. Erdman, Jr., and W. D. O'Brien, Jr., "Ultrasonic attenuation and velocity properties in rat livers as a function of fat content - study at 100 MHz using a scanning laser acoustic microscope," *J. Acoust. Soc. Am.*, vol. 77, pp. 307-313, 1985.

Kalervo M. U. Tervola was born in Kälviä, Finland, on July 29, 1956. He received his B.S. and M.S. degrees in electrical engineering from the University of Oulu, Finland, in 1979 and 1982, respectively.

From 1979 to 1981 he served as Teaching Assistant at the University of Oulu. From 1982 to 1983 he worked as a Research Assistant and since 1984 as a Junior Researcher in the Academy of Finland. He was with the Bioacoustics Research Laboratory at the University of Illinois, developing tissue characterization techniques and studying the ultrasonic propagation properties of tissues using a 100 MHz scanning laser acoustic microscope. His main research interests deal with acoustical imaging.

Steven G. Foster, photograph and biography not available at the time of publication.

William D. O'Brien, Jr. (S'64-M'71-SM'79), for a photogrtaph and biography see page 25 of the January 1985 issue of this TRANSACTIONS.